Journal of Statistical Physics, Vol. 70, Nos. 1/2, 1993

Chaotic Resonance: A Simulation

Erich Ippen,[1] John Lindner,[1] and William L. Ditto[1]

Stochastic resonance is a statistical phenomenon that has been observed in periodically modulated, noise-driven, bistable systems. The characteristic signatures of the effect include an increase in the signal-to-noise of the output as noise is added to the system, and exponentially decreasing peaks in the probability density as a function of residence times in one state. Presented are the results of a numerical simulation where these same signatures were observed by adding a *chaotic* driving term instead of a white noise term. Although the probability distributions of the noise and chaos inputs were significantly different, the stochastic and chaotic resonances were equal within the experimental error.

KEY WORDS: Chaos; resonance; stochastic.

1. INTRODUCTION

Stochastic resonance (SR) is a statistical phenomenon observed in bistable systems that are modulated with both a periodic and a noise drive term. When the sum of the amplitudes of the drive terms is great enough, the system may switch between the two stable states. Since the switching is dependent on both driving terms, the time intervals between switches are related to the periodic modulation signal. Their relationship depends on the amplitude of the random noise term. For some amplitudes of noise the switching of the system will be very closely related to the modulation signal.

Two characteristic signatures of stochastic resonance are the increase of the output signal-to-noise ratio (SNR) as noise is increased and a specific probability density of residence times in a given state. If switching between the states is purely random, driven only by noise, then the probability of the system residing in one state for a given amount of time

[1] Department of Physics, College of Wooster, Wooster, Ohio 44691.

0022-4715/93/0100-0437$07.00/0

decreases exponentially as a function of residence time. As a periodic signal is added, switching correlated with the periodic signal occurs. The system tends to remain in one state for times equal to half-integer multiples of the driving period.[1]

2. CHAOTIC RESONANCE

In many physical systems in which stochastic resonance is studied, the dynamics causing the switching may be modeled by an overdamped particle in a continuous double-well potential.[2] Restrict the particle to a quartic potential curve given by the equation

$$U(x) = +k\frac{x^2}{2} - k'\frac{x^4}{4}, \qquad k, k' < 0 \tag{1}$$

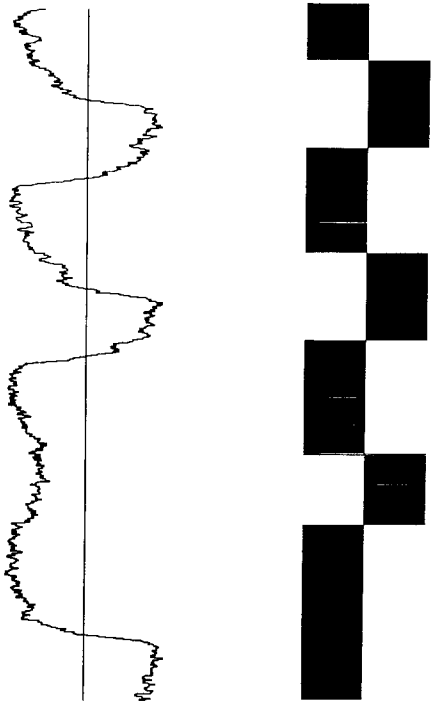

Fig. 1. Time series output of Eq. (5). Time is vertical and amplitude is horizontal. Unfiltered motion (left) and filtered motion (right) are for different runs. The filtered motion exhibits some anomalous switching events.

Add a viscous drag, a periodic modulation, and white noise. The total force on the particle is

$$m\ddot{x} = F(x) = -kx + k'x^3 - b\dot{x} + A\sin(\omega t) + A'\xi(t) \tag{2}$$

In the limit of large damping, neglect the inertial term $m\ddot{x}$ and absorb the damping constant b to get the overdamped stochastic Duffing equation[1]

$$\dot{x} = -kx + k'x^3 + A\sin(\omega t) + A'\xi(t) \tag{3}$$

Propagation of this equation yields a time series governing the position x of the particle. The output of the time series is a result of the two time-dependent elements of Eq. (3), the noise term and the periodic term. To observe stochastic resonance, the periodic term must be weak enough that in the absence of noise, no switching can occur. Note that for zero noise input, the time series depends only on the sinusoidal term.

Since we are simulating a two-state system, we filter the output time series so that the output is $+1$ if x is positive and -1 if x is negative. All intrawell motion is ignored. (Refer to Fig. 1.) This corresponds to the digi-

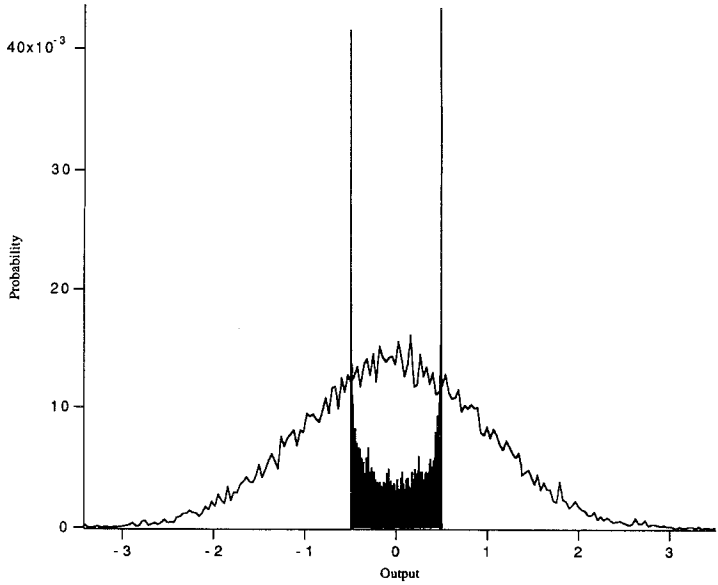

Fig. 2. Probability distributions of the logistic map output, adjusted to $[-1/2, +1/2]$ (black), and the white noise output (white).

tal output of a Schmitt trigger or to the direction of lasing in a ring laser.[1] The Fourier transform of the output time series extracts the frequency of modulation. Data taken from the power spectral density (PSD), the absolute square of the Fourier transform, yields the characteristic SNR curve. The PSD of the output contains a series of spikes (in theory, Dirac deltas[2] at odd integer multiples of the modulation frequency, against a background of noise). If no switching occurs, there will be no signal in the output time series and the SNR will be zero.

Typically the switching between wells has been induced with broadband "white" noise, that is, noise whose probability distribution is Gaussian (with unit variance and zero mean). The probability distribution of our simulation's noise generator[3] is shown in Fig. 2. This output $\xi(t)$ was multiplied by an amplitude A' to determine the kick $A'\xi(t)$ given to the particle. [Refer to Eq. (3).] We have shown that it is possible to induce switching using a *chaos* term, specifically, the output of the logistic map,[4] rather than a noise term.

The chaotic driving term is obtained by iterating the logistic map. The logistic map gives a discrete time series of numbers on the interval [0, 1] which, for certain parameters, vary chaotically. For a given seed x_n, the next value in the series is given by

$$x_{n+1} = 4\lambda x_n(1 - x_n) \tag{4}$$

Depending on the parameter λ and on the initial input seed, the time series may converge to a periodic or a chaotic attractor. In our simulation, λ was set to 1, a value well known to yield a chaotic attractor. The initial value x_n was 0.123456789. (Certain inputs, for example, 0, 1, 0.25, 0.5, 0.75, are stable and do not result in chaos, so it was necessary to choose an initial point that would not yield a trivial solution.) Furthermore, the output is not immediately chaotic and it is often necessary to iterate Eq. (4) many times before the output finally frees itself from transient states and settles on the attractor. For our simulation, the output was not used as a driving term until the logistic map was iterated 1000 times.

The output of the logistic map is a chaotic set of numbers between 0 and 1. In order to have an output that caused switching between both wells, we scaled the output to lie between $-1/2$ and $+1/2$. The probability distribution of this output is compared to the Gaussian noise distribution in Fig. 2. Both distributions were obtained experimentally from the output of the simulation. The logistic distribution has a zero mean; however, the most probable outputs are close to $\pm 1/2$, in contrast to the Gaussian, whose most probable output is zero. The output from the logistic map $\chi(t)$ was multiplied by an amplitude A'' to determine the kick $A''\chi(t)$ given to

Table I. Definitions of Data-Taking Regions

Parameter	Region 1	Region 2	Region 3
k	−2.1078	−5.000	−3.3824
k'	−1.4706	−1.1373	−2.7387
A	1.3039	4.700	1.775
ω	0.7304	0.8900	0.8039

the particle. [Refer to Eq. (5).] The rate of switching was controlled by changing this amplitude.

For the equation

$$\dot{x} = -kx + k'x^3 + A\sin(\omega t) + A'\xi(t) + A''\chi(t) \tag{5}$$

the regions which we used in taking data are described in Table I.

Equation (5) was integrated using a fourth-order Runge-Kutta routine.[3] The time step τ was originally set to be 1/50th of the driving period. For large noise values this approximation was no longer good enough and the simulation would diverge. For this reason, the time step τ was halved to 1/100th of the driving period. This worked well for region 1, but in the higher noise values of region 2, the approximation again failed and the time step had to be halved again.

3. ANALYSIS OF SIMULATION DATA

For a series of noise inputs the simulation program calculated the power spectrum of the filtered time series using a fast Fourier transform.[3] The noise inputs were meant to cover the essential range of the output SNRs (initial increase, resonance, and gradual decrease), but it was necessary to resolve the maximum so that stochastic and chaotic resonances might be compared. The PSD averaged $2k$ segments of $2M$ points each, where k and M are each powers of 2. For the data presented, $M = 2^{13}$ and $k = 2^4$.

The PSDs displayed a series of peaks at odd integer multiples of the driving frequency. The first peak (located at the driving frequency) was, however, by far the largest. For region 1, the peak was contained in essentially two adjacent bins (out of $2^{13} = 8192$ bins total in the PSD). The noise level at the driving frequency was measured by averaging the values for the three bins to the left of the signal peak and the three bins to the right. The error in the measurement of the peak height was estimated at about ± 0.001, while the error in the output noise level was the standard

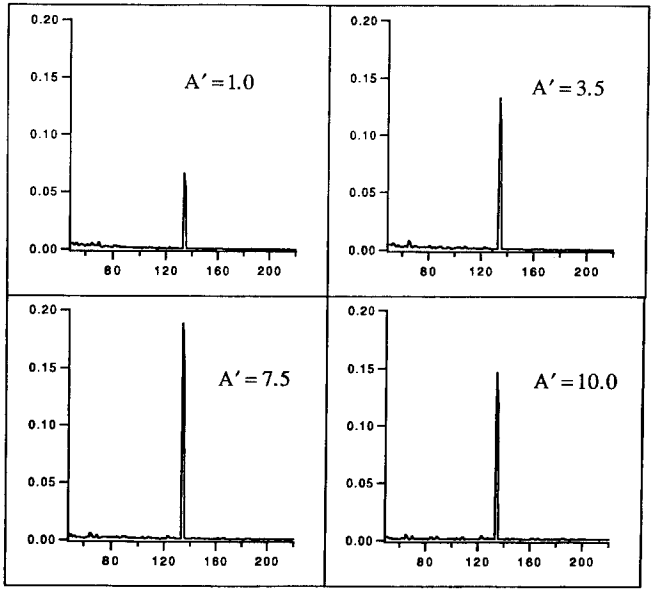

Fig. 3. PSDs (from region 1) as the noise amplitude A' is varied.

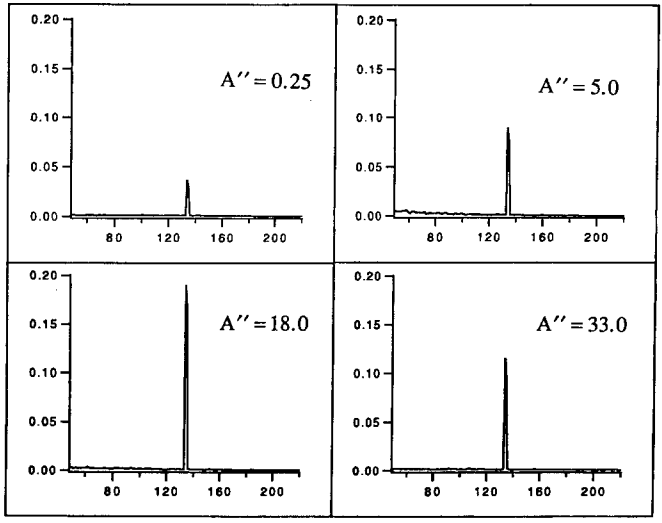

Fig. 4. PSDs (from region 3) as the chaos amplitude A'' is varied.

deviation of the six measured noise values. This was in general around ± 0.0002, although for very low input noise this was slightly less.

The resulting signal peaks and noise values were used to plot SNR as a function of input noise, where the SNR was defined as

$$\mathrm{SNR} = 10 \log_{10}\left(1 + \frac{\text{signal}}{\text{noise}}\right) \tag{6}$$

in decibels. The error in the SNR is due mainly to the standard deviation of the noise levels. The scatter is generally a result of noise levels differing by as little as 0.0001. Bin leakage posed a problem in measuring the noise levels directly adjacent to the bins containing the signal peak. In region 2, the peak was contained in at least three, and possibly four, bins. Measurement of the noise level required taking data from bins at least two bins away from the signal peak. Figures 3 and 4 are representative of the data.

4. RESULTS

Region 1 was the first to be investigated because it combines a very small modulation amplitude with a phase space orbit that is very close to switching. This means that the region is very prone to switching, but also that the signal may be obscured without drastic amounts of noise or chaos. The results of the noise- and chaos-induced resonances are shown in Figs. 5 and 6, respectively. (We attempted to resolve little else than the resonance.)

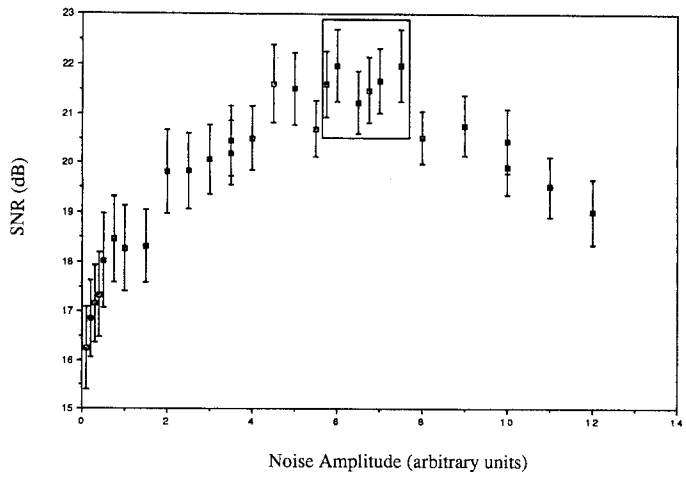

Fig. 5. SNR versus noise amplitude in region 1. The resonance is at 21.7 ± 0.2 and the maximum SNR is 22.0 ± 0.7 dB.

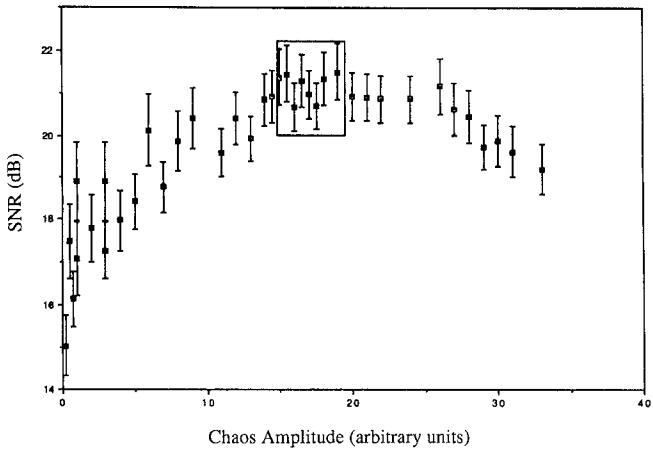

Fig. 6. SNR versus chaos amplitude in region 1. The resonance is at 21.2 ± 0.3 and the maximum SNR is 21.5 ± 0.7 dB.

The stochastic resonance (SR) is apparently contained within the six data points, while the slightly denser plot of the chaotic resonance (CR) shows approximately eight points that could be construed as belonging to the resonance (Table II).

The average SNR is 21.7 ± 0.2 dB for the SR and 21.2 ± 0.3 dB for the CR. The chaos-induced resonance is only slightly less than the stochastic, the difference being within the experimental error. The absolute heights of the stochastic and chaotic curves are 22.0 ± 0.7 dB and 21.5 ± 0.7 dB, respectively. These are the same within the experimental error, as summarized in Table IV. One qualitative difference between the data forming the two curves is that the chaotic resonance data are much more scattered, particularly for low chaos inputs.

Table II. Stochastic Resonance versus Chaotic Resonance in Region 1

Noise A'	SNR (dB)	Chaos A''	SNR (dB)
5.75	21.6 ± 0.7	15.0	21.4 ± 0.7
6.0	22.0 ± 0.7	15.5	21.5 ± 0.7
6.5	21.2 ± 0.6	16.0	20.7 ± 0.6
6.75	21.5 ± 0.7	16.5	21.3 ± 0.6
7.0	21.7 ± 0.6	17.0	21.0 ± 0.6
7.5	22.0 ± 0.7	17.5	20.7 ± 0.5
		18.0	21.4 ± 0.6
		19.0	21.5 ± 0.7

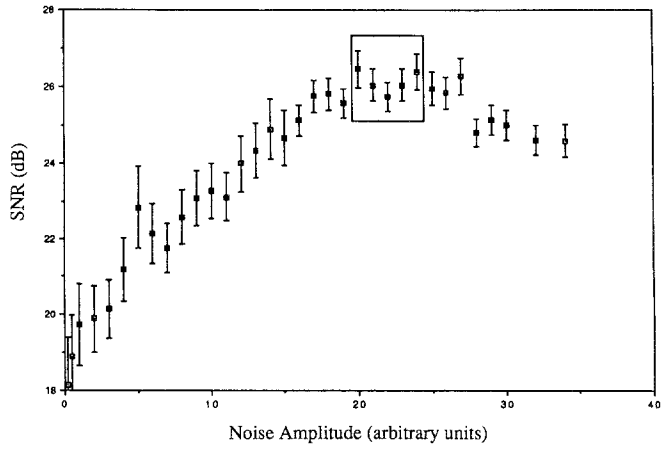

Fig. 7. SNR versus noise amplitude in region 2. The resonance is at 26.1 ± 0.3 and the maximum SNR is 26.5 ± 0.5 dB.

Region 2 has a larger amplitude and deeper wells than region 1, hence the resonance is more robust. That is, it is more difficult to observe a decrease in the SNR. Furthermore, a zero-noise/chaos phase-space plot shows that it is not as close to switching, so more noise/chaos is required to induce switching.

The results of the PSDs are shown in Figs. 7 and 8, where the SNR is plotted versus the noise and chaos amplitudes. The CR was found by

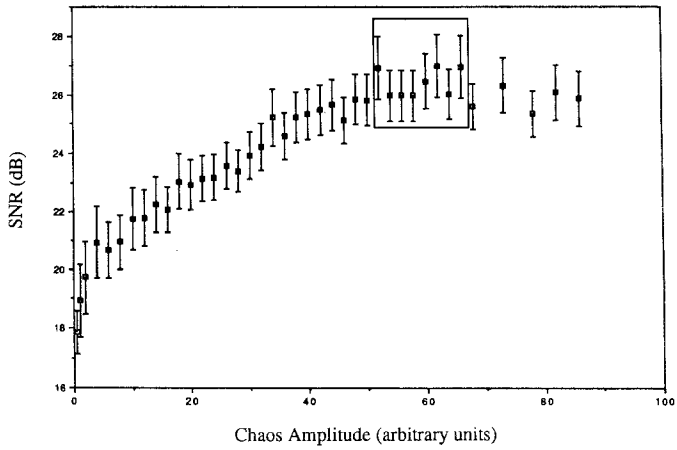

Fig. 8. SNR versus chaos amplitude in region 2. The resonance is at 26.4 ± 0.4 and the maximum SNR is 27 ± 1 dB.

Table III. Stochastic Resonance versus Chaotic Resonance in Region 2

Noise A'	SNR (dB)	Chaos A''	SNR (dB)
20.0	26.5 ± 0.5	52.0	26.9 ± 1.0
21.0	26.0 ± 0.4	54.0	26.0 ± 0.9
22.0	25.7 ± 0.4	56.0	26.0 ± 0.9
23.0	26.0 ± 0.4	58.0	26.0 ± 0.9
24.0	26.4 ± 0.5	60.0	26.5 ± 1.0
		62.0	27.0 ± 1.0
		64.0	26.0 ± 0.9
		66.0	27.0 ± 1.0

averaging eight points which appeared to contain the resonance. The SR was, likewise, the average of five resonance points (Table III).

The average of these points yielded an SR of 26.1 ± 0.3 dB and a CR of 26.4 ± 0.4 dB. Again, the magnitudes of the resonances are equivalent to within the experimental error.

If the SR is slightly below the CR, it is probably due to an interesting artifact that appeared in the PSDs of the SR time series. The noise level was calculated by averaging six bins of the PSD (three bins to the right

Table IV. Summary of Regions 1, 2, and 3 at Resonance

	Noise	Chaos
Region 1		
Avg SNR	21.7 ± 0.2	21.2 ± 0.3
Max SNR	22.0 ± 0.7	21.5 ± 0.7
Avg PSD	18.7 ± 0.2	18.4 ± 0.5
Max PSD	18.8 ± 0.1	18.8 ± 0.1
Avg PSD	1300 ± 100	1400 ± 100
Region 2		
Avg SNR	26.1 ± 0.3	26.4 ± 0.4
Max SNR	26.5 ± 0.5	27.0 ± 1.0
Avg PSD	39.9 ± 0.2	39.6 ± 0.2
Max PSD	40.1 ± 0.1	39.8 ± 0.1
Avg PSD	1000 ± 100	900 ± 100
Region 3		
Avg SNR	21.9 ± 0.3	21.7 ± 0.9
Max SNR	22.2 ± 0.1	22.2 ± 0.6
Avg PSD	34.8 ± 0.7	34.7 ± 0.5
Max PSD	36.1 ± 0.1	36.1 ± 0.1
Avg PSD	2200 ± 100	2100 ± 100

and left of the spike). In the bin farthest to the right of the spike, a lump appeared that was slightly higher than the noise level in the adjacent bins. This occurred only for the noise-induced switching and even then it was only apparent at higher noise inputs. Around the resonance, this bin was almost a factor of two greater than the surrounding bins.

Even so, the maximum SNRs were equivalent within the error. If the five SNRs corresponding to the SR are recalculated and averaged, excluding this one bin, then the resonance is approximately 26.6 ± 0.2, slightly larger than than but still close to the CR. The CR induced a maximum peak of 39.8 ± 0.01 as compared to the SR, which attained 40.1 ± 0.01. Refer to Table IV. Notice that the noise levels for the SR are slightly larger than those for the CR. This is likely a result of the artifact mentioned above.

Finally, we investigated a region lying somewhere between the previous two. The frequency and amplitude are slightly greater than those for region 1; however, they are considerably less than those for region 2. A zero-noise phase-space orbit shows that it is closer to switching than region 2, which means that the maximum SNR may be obtained with less noise/chaos input. The orbit is most similar to that of region 1.

The average noise levels are almost equivalent and the results of the SNR plots were similar to those obtained for the previous two regions. This is summarized in Table VI. Figures 9 and 10 show the SNR plots where the apparent resonance points are boxed. The average SNR for the SR was 21.9 ± 0.3 dB, compared with 21.7 ± 0.9 dB for the CR.

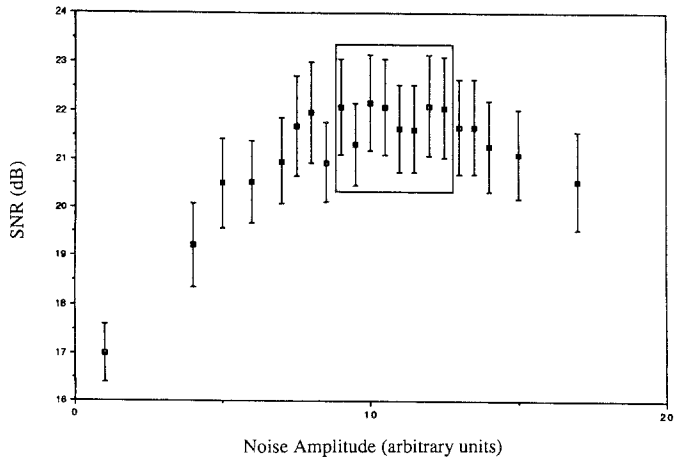

Fig. 9. SNR versus noise amplitude in region 3. The resonance is at 21.9 ± 0.3 and the maximum SNR is 22.2 ± 1.0 dB.

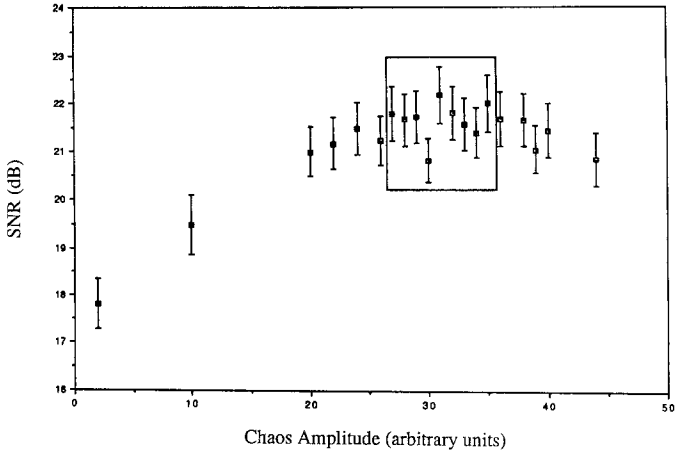

Fig. 10. SNR versus chaos amplitude in region 3. The resonance is at 21.7 ± 0.3 and the maximum SNR is 22.2 ± 0.6 dB.

5. RESIDENCE TIME DISTRIBUTIONS

One of the defining characteristics of stochastic resonance is the residence time probability distribution. In region 2, dwell-time data were taken for stochastic as well as chaotic resonance. The distributions are shown in Figs. 11 and 12. The SR distribution shows the expected series of exponentially decreasing peaks, but also some unexplained gaps (corresponding to zero probability) appearing within the spikes. This discrepancy may be a result of the fact that there was no hysteresis in the switching process: Whenever the particle crossed the vertical axis, the filtered output would switch. This led to a number of anomalous switching events where the particle would cross the center point and, without actually falling into the opposite well, would be immediately pushed back into the original well. (Refer to Fig. 1.) These very short switches must have affected the probability distribution. Introducing a hysteresis might correct for this problem. To investigate this matter further would also require a finer binning of the probability histogram (the simulation binned the data in only 128 bins). However, the CR yields a probability distribution that is qualitatively equivalent to the SR dwell-time distribution. (Refer to Figs. 11 and 12.)

6. CONCLUSION

A SNR increase in the output of a bistable system is the defining feature of stochastic resonance. It can be seen in Figs. 3–12 that chaos can

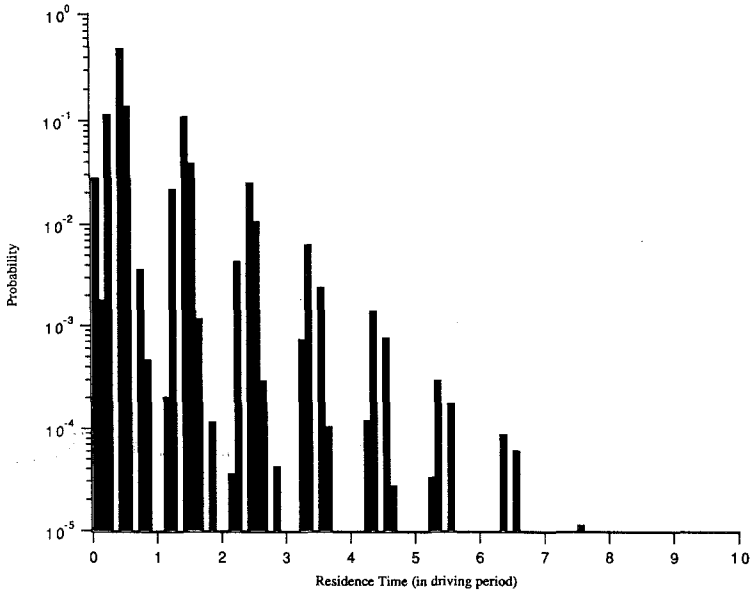

Fig. 11. SR residence time probability distributions with noise amplitude $A' = 5.0$. The series of spikes of exponentially decreasing heights (linear on the log scale) occur at odd multiples of the half period of forcing.

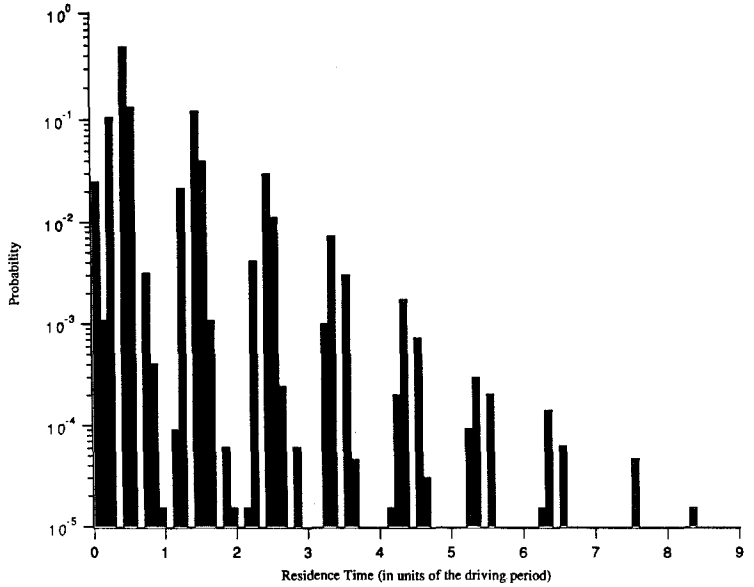

Fig. 12. CR residence time probability distributions with chaos amplitude $A'' = 13.0$. Again, the series of spikes of exponentially decreasing heights (linear on the log scale) occur at odd multiples of the half period of forcing.

induce this effect just as easily as white noise. While the precise shapes of the SNR curves may differ, they exhibit the same broad features: steep increase in the SNR, resonance, and then a gradual decrease. Furthermore, the resonances are practically equivalent. The peak values of Table IV are equal to within the experimental error. The implication of this is that white noise and the logistic map, despite having drastically different probability distributions, produce nearly the same effect. (An important similarity between the two distributions is that both are symmetric about zero, provided the logistic map is scaled to the interval $[-1/2, +1/2]$.)

Any difference between the two resonances is difficult to observe in the individual SNR curves. Table IV may, however, provide some insight as to general overall trends. The signal-to-noise ratios, calculated from Eq. (6), are quite sensitive to small changes in the noise level. It may be more useful, when comparing stochastic to chaotic resonance, to look at the average heights of the spikes in the PSDs while at resonance. It can be seen from Table IV that, although all discrepancies are within the experimental error, the average height of the SR peaks is consistently, albeit slightly, greater than that of the average CR peaks. This would mean that stochastic resonance is somewhat stronger than the logistic-map-generated chaotic resonance. To prove this would require more statistics.

An aspect that deserves further investigation is the effect of introducing a hysteresis to the switching. There remain unexplained gaps in the residence time probability distribution that may relate to this. The effect that this would have on the PSDs could be even more important. Finally, we have investigated CR with only one form of chaos: the logistic map, which provides a symmetric and continuous distribution of kicks to the system. Other chaotic terms, possibly with asymmetric or discrete probability distributions, may yield more insight into the nature of stochastic and chaotic resonance.

REFERENCES

1. F. Moss, Stochastic resonance, preprint (January 1992).
2. T. Zhou and F. Moss, *Phys. Rev. A* **41**:4255 (1990).
3. W. Press, B. Flannery, S. Teukolsky, and W. Vetterling, *Numerical Recipes in C* (Cambridge University Press, Cambridge, 1988).
4. I. Percival and D. Richards, *Introduction to Dynamics* (Cambridge University Press, Cambridge, 1982).